ELSEVIER

Engineering Analysis with Boundary Elements 31 (2007) 259–266

ENGINEERING ANALYSIS with BOUNDARY ELEMENTS

www.elsevier.com/locate/enganabound

3-D boundary element–finite element method for velocity–vorticity formulation of the Navier–Stokes equations

Zoran Žunič*, Matjaž Hriberšek, Leopold Škerget, Jure Ravnik

Institute of Power, Process and Environmental Engineering, Faculty of Mechanical Engineering, University of Maribor, Smetanova ulica 17, 2000 Maribor, Slovenia

Received 29 November 2005; accepted 6 September 2006
Available online 24 October 2006

Abstract

A numerical method for the solution of the incompressible Navier–Stokes equations was developed using an integral representation of the conservation equations. The velocity–vorticity formulation is employed, where the kinematics is given with the Poisson equation for the velocity vector, while the kinetics is represented with the vorticity transport equation. Based on computational aspects, resulting from CPU time and memory requirements of the boundary domain integral method, a combined approach to the solution of the set of governing equations is proposed. Kinematics is solved using boundary element method (BEM), while kinetics is solved using finite element method (FEM). Lid driven flow in a cubic cavity was considered to show the robustness and versatility of this formulation. Results of $Re = 100, 400, 1000$ show a good agreement with benchmark results.

Keywords: 3-D incompressible viscous fluid flow; Velocity–vorticity formulation; Boundary element method; Finite element method; Lid driven cavity

1. Introduction

The research in the field of numerical algorithms for computation of viscous fluid flow mainly focuses on the development of approximation methods for the solution of the Navier–Stokes equations. The majority of approaches use only one type of approximation method, like finite difference (FDM), finite volume (FVM), finite element (FEM) or boundary element methods (BEMs). Since each of those methods has some favorable and some unfavorable properties, a lot of research was also done in the development of mixed approximation methods.

Velocity–vorticity approach attracted several researchers to make their contributions to the field, among others Liu [1] used finite differences to solve $\vec{v} - \vec{\omega}$ formulation and Guevremont et al. [2,3] and Wong and Baker [4] used finite element approach.

In the context of BEM-based velocity–vorticity formulation, work of Žagar and Škerget [5] was one of the first attempts to solve three-dimensional viscous laminar flow by BEM. Hriberšek and Škerget [6] and Škerget et al. [7] later indicated that the solution of flow kinematics equation is of main importance for assuring mass conservation property of the numerical algorithm. The solution of Poisson velocity equation for flow kinematics by BEM leads to a better numerical scheme with the respect of mass conservation, regardless of the discretisation approach in flow kinetics.

Several researchers also worked on combination of boundary element and finite element methods. In the field of viscous fluid flow numerical simulation, an important work was done by Young et al. [8] using primitive variable formulation of Navier–Stokes equations. They computed pressure field with BEM and momentum equation with three step FEM. In the field of viscous fluid flow numerical simulation with velocity–vorticity formulation of Navier–Stokes equations the contributions were made by Young et al. [9], where BEM was used to obtain boundary velocities and normal velocity fluxes implicitly and then explicitly the internal velocities and boundary vorticities were computed by derivation of kinematic integral equations. Slightly different approach was used by Brown and Ingber [10] and Brown et al. [11] where internal

*Corresponding author. Tel.: +386 2 220 7777; fax: +386 2 220 7990.
E-mail address: zoran.zunic@uni-mb.si (Z. Žunič).

0955-7997/$ - see front matter © 2006 Elsevier Ltd. All rights reserved.
doi:10.1016/j.enganabound.2006.09.001

velocities were computed using regular form of generalised Helmholtz decomposition and boundary conditions for vorticity transport equation were applied using vortex sheet strengths. Vorticity transport equation was solved with Galerkin FEM. Combined algorithm was also used by Žunič et al. [12], where the detailed comparison of different approaches to computation of internal velocities was presented.

Present work is a combination of BEM-based solution of vector Poisson velocity equation for computation of boundary vorticities and FEM-based solution of Poisson velocity equation for computation of internal velocities and for solution flow kinetics. The former allows implicit computation of vorticity values at the solid walls, and the latter is chosen in order to avoid the use of macro element-based subdomain technique in BEM, which is numerically accurate and stable, but results in a larger system of linear equations for flow kinetics due to use of discontinuous elements, Škerget et al. [13] or due to use of mixed boundary element types, Ramšak et al. [14]. The FEM discretisation is computationally less demanding and is therefore used in our numerical algorithm. Although the solution of kinematics equation for internal velocities could be obtained by an explicit BEM calculation, we were forced at this stage of research to use FEM in order to meet the computer memory requirements. However, the research in the field of subdomain BEM for solving transport equations is still continuing.

2. Velocity–vorticity formulation of Navier–Stokes equations

The analytical description of the motion of a continuous fluid is based on conservation of mass and momentum

$$\vec{\nabla}\cdot\vec{v}=0, \tag{1}$$

$$\frac{\partial\vec{v}}{\partial t}+(\vec{v}\cdot\vec{\nabla})\vec{v}=-\frac{1}{\rho}\vec{\nabla}p+\nu\nabla^2\vec{v}, \tag{2}$$

where ρ is fluid density and ν is kinematic viscosity of the fluid, which are both constant throughout the domain.

The dynamics of a viscous incompressible fluid flow is partitioned into its kinematic and kinetic aspect through the use of derived vector vorticity field function, see Škerget et al. [7] and Ravnik et al. [15].

Vorticity $\omega_i(r_j,t)$ is defined as a curl of the velocity field $v_i(r_j,t)$

$$\vec{\omega}=\vec{\nabla}\times\vec{v},\quad \vec{\nabla}\cdot\vec{\omega}=0, \tag{3}$$

resulting in the following elliptic Poisson equation for the velocity vector

$$\nabla^2\vec{v}+\vec{\nabla}\times\vec{\omega}=0. \tag{4}$$

Vorticity kinetics is governed by vorticity transport equation, which is obtained as a curl of momentum Eq. (2) and may be, in the case of incompressible viscous fluid flow, written as

$$\frac{\partial\vec{\omega}}{\partial t}+(\vec{v}\cdot\vec{\nabla})\vec{\omega}=(\vec{\omega}\cdot\vec{\nabla})\vec{v}+\nu\nabla^2\vec{\omega}. \tag{5}$$

We seek a solution of Eqs. (4) and (5) in the domain Ω, which satisfies the initial conditions

$$\vec{v}=\vec{v}_0,\quad \vec{\omega}=\vec{\omega}_0=\vec{\nabla}\times\vec{v}_0,\quad \text{at } t=0 \tag{6}$$

and the boundary conditions

$$\vec{v}=\vec{v}_\Gamma,\quad \vec{\omega}=(\vec{\nabla}\times\vec{v})|_\Gamma,\quad \text{at } t\geqslant 0 \tag{7}$$

on the boundary Γ of the domain Ω.

As described in the introduction, the paper deals with numerical solution of flow kinematics by means of BEM and computation of internal velocities in flow kinematics and vorticities in flow kinetics by means of FEM.

3. Integral form of the governing equations

In this section, we will describe the integral representation of governing equations written in previous section in the form of partial differential equations. We will start with collocation integral equation of kinematics followed by Galerkin weak formulation of kinematics and finally Galerkin weak formulation of kinetics.

3.1. Boundary element integral representation of kinematics

The singular boundary integral representation for the velocity vector can be formulated by using the Green theorems for scalar functions, or weighting residuals technique. The integral form of Poisson-type equation [16,17] is used on the kinematic Eq. (4), yielding

$$c(\xi)\vec{v}(\xi)+\int_\Gamma \vec{v}(\vec{n}\cdot\vec{\nabla})u^\star\,\mathrm{d}\Gamma=\int_\Gamma u^\star(\vec{n}\cdot\vec{\nabla})\vec{v}\,\mathrm{d}\Gamma+\int_\Omega(\vec{\nabla}\times\vec{\omega})u^\star\,\mathrm{d}\Omega, \tag{8}$$

with $u^\star=u^\star(\xi,S)$ denoting the elliptic Laplace fundamental solution, ξ is the source point on boundary Γ, S integration point in domain Ω (including Γ), $c(\xi)$ geometry coefficient and $\vec{n}$ outward pointing normal to the boundary. Geometry coefficient can be generally computed as $\Theta/4\pi$, where Θ is the internal solid angle at point ξ in steradians. Laplace fundamental solution is

$$u^\star(\xi,S)=\frac{1}{4\pi r(\xi,S)}, \tag{9}$$

where $\xi\in\Gamma$ is source point, $S\in\Omega$ is integration point and r distance between the source and the integration point.

In order to avoid the derivatives of the velocity and vorticity fields in Eq. (8) the derivatives in the integral kinematics equation are transferred to the fundamental solution. The Gauss divergence clause and the solenoidality constraint are used. The derivation is described in detail in Škerget et al. [7] and Ravnik et al. [15]. The final integral form of the kinematics equation, employing the derivatives

of the fundamental solution, reads:

$$c(\xi)\vec{v}(\xi)+\int_{\Gamma}(\vec{\nabla}u^{\star}\cdot\vec{n})\vec{v}\,\mathrm{d}\Gamma=\int_{\Gamma}(\vec{\nabla}u^{\star}\times\vec{n})\times\vec{v}\,\mathrm{d}\Gamma+\int_{\Omega}\vec{\omega}\times\vec{\nabla}u^{\star}\,\mathrm{d}\Omega. \tag{10}$$

3.2. Finite element integral representation of kinematics

Following the Galerkin weighted residual method [18,19] we multiply Eq. (4) by the weighting function N and integrate it over the domain, to obtain

$$\int_{\Omega}N\nabla^{2}\vec{v}\,\mathrm{d}\Omega+\int_{\Omega}N(\vec{\nabla}\times\vec{\omega})\,\mathrm{d}\Omega=0. \tag{11}$$

Next we apply Green's first theorem to the diffusion term to obtain a weak formulation of kinematic Poisson equation as

$$\int_{\Omega}\vec{\nabla}N\cdot\nabla\vec{v}\,\mathrm{d}\Omega-\int_{\Gamma}N(\vec{n}\cdot\vec{\nabla}\vec{v})\,\mathrm{d}\Gamma-\int_{\Omega}N(\vec{\nabla}\times\vec{\omega})\,\mathrm{d}\Omega=0. \tag{12}$$

3.3. Finite element integral representation of vorticity transport equation

Equivalent procedure can be performed to obtain weak formulation of vorticity transport equation. We multiply Eq. (5) by the weighting function N and integrate it over the domain Ω, to obtain

$$\int_{\Omega}N\frac{\partial\vec{\omega}}{\partial t}\,\mathrm{d}\Omega+\int_{\Omega}N(\vec{v}\cdot\vec{\nabla})\vec{\omega}\,\mathrm{d}\Omega=\int_{\Omega}N(\vec{\omega}\cdot\vec{\nabla})\vec{v}\,\mathrm{d}\Omega+\nu\int_{\Omega}N\nabla^{2}\vec{\omega}\,\mathrm{d}\Omega. \tag{13}$$

Replacing time derivative with first-order backward finite differences approximation

$$\frac{\partial\vec{\omega}}{\partial t}=\frac{\vec{\omega}-\vec{\omega}_{\tau-1}}{\Delta t} \tag{14}$$

and applying Green's first theorem to the diffusion term, one can obtain a weak formulation of kinetic equation

$$\frac{1}{\Delta t}\int_{\Omega}N\vec{\omega}\,\mathrm{d}\Omega+\int_{\Omega}N(\vec{v}\cdot\vec{\nabla})\vec{\omega}\,\mathrm{d}\Omega=\int_{\Omega}N(\vec{\omega}\cdot\vec{\nabla})\vec{v}\,\mathrm{d}\Omega-\nu\int_{\Omega}\vec{\nabla}N\cdot\vec{\nabla}\vec{\omega}\,\mathrm{d}\Omega+\nu\int_{\Gamma}N(\vec{n}\cdot\vec{\nabla}\vec{\omega})\,\mathrm{d}\Gamma+\frac{1}{\Delta t}\int_{\Omega}N\vec{\omega}_{\tau-1}\,\mathrm{d}\Omega, \tag{15}$$

where Δt is the size of time step and subscript $\tau-1$ denotes vorticity value in previous time step.

4. Discrete form of equations

To obtain discrete form of integral equations we divide computational domain Ω into elements Ω_e and the field function variation within the element e is described with

$$u^{e}(S)=\sum_{n=1}^{np}N_{n}^{e}(S)U_{n}^{e}, \tag{16}$$

where S is point inside the element Ω_e, np is the number of nodal points of the element, N_n^e are interpolation functions, U_n^e are nodal values of variable u for the element Ω_e and u stands for components of velocity v_i or vorticity ω_i.

Final interpolation function for node jn is

$$N_{jn}=\sum_{e=1}^{N_{ce}}N_{n}^{e}, \tag{17}$$

where n is the local node number of node jn in element e and N_{ce} is the number of elements which contain node jn.

For interpolation of domain values we use eight-point hexahedrons with trilinear interpolation functions and for interpolation of boundary values four-point quadrilateral elements with bilinear interpolation functions.

4.1. Discrete form of BEM kinematics

The use of interpolation functions N (17) for geometry and field functions representation in Eq. (10), leads us to

$$\begin{aligned}[H]\{V_x\}&=[H_{z,x}]\{V_z\}-[H_{x,y}]\{V_y\}+[D_z]\{W_y\}-[D_y]\{W_z\},\\ [H]\{V_y\}&=[H_{x,y}]\{V_x\}-[H_{y,z}]\{V_z\}+[D_x]\{W_z\}-[D_z]\{W_x\},\\ [H]\{V_z\}&=[H_{y,z}]\{V_y\}-[H_{z,x}]\{V_x\}+[D_y]\{W_x\}-[D_x]\{W_y\},\end{aligned} \tag{18}$$

where matrices of integrals are defined as

$$H^{in,jn}=\sum_{e=1}^{be}\int_{\Gamma_e}\left(\frac{\partial u^{\star}(\xi_{in},S_{\Gamma_e})}{\partial x_i}n_i\right)N_{jn}\,\mathrm{d}\Gamma\ +\delta(in,jn)c(\xi_{in}), \tag{19}$$

$$H_{i,j}^{in,jn}=\sum_{e=1}^{be}\int_{\Gamma_e}\left(\frac{\partial u^{\star}(\xi_{in},S_{\Gamma_e})}{\partial x_i}n_j-\frac{\partial u^{\star}(\xi_{in},S_{\Gamma_e})}{\partial x_j}n_i\right)N_{jn}\,\mathrm{d}\Gamma, \tag{20}$$

$$D_{i}^{in,jn}=\sum_{e=1}^{ne}\int_{\Omega_e}\frac{\partial u^{\star}(\xi_{in},S_{\Gamma_e})}{\partial x_i}N_{jn}\,\mathrm{d}\Omega \tag{21}$$

and $u^{\star}(\xi_{in},S_{\Gamma_e})$ is the elliptic Laplace fundamental solution, function $\delta(in,\ jn)$ has value 1 for $in=jn$ and value 0 for $in\neq jn$, indices in and jn denote the row and column position of integral in matrix (node numbers of the source and destination node in discretised domain), $[H]$ is matrix of boundary integrals of normal derivatives of fundamental solution, $[H_{i,j}]$ are matrices of boundary integrals of tangential derivatives of fundamental solution and $[D_i]$ are matrices of domain integrals of gradient of fundamental solution. Indices i and j denote the x, y and z coordinates.

The number of rows in all matrices is equal to the number of boundary nodes ($in\in[1,N_{\Gamma}]$). The number of columns in boundary matrices (Eqs. (19) and (20)) and the size of velocity vector $\{V_i\}$ is also equal to the number of

boundary nodes ($jn \in [1, N_\Gamma]$), while the number of columns in the domain matrices (21) and the size of vorticity vector $\{W_i\}$ is equal to the number of domain nodes ($jn \in [1, N_\Omega]$).

In order to obtain better conditioned system matrix for computation of boundary vorticities we transform the discretised equations (18) into tangential form. We perform a vector product of (18) by normal vector

$$\begin{Bmatrix} [n_x] \\ [n_y] \\ [n_z] \end{Bmatrix} \times \begin{Bmatrix} [H]\{V_x\} - [H_{zx}]\{V_z\} + [H_{xy}]\{V_y\} - [D_z]\{W_y\} + [D_y]\{W_z\} \\ [H]\{V_y\} - [H_{xy}]\{V_x\} + [H_{yz}]\{V_z\} - [D_x]\{W_z\} + [D_z]\{W_x\} \\ [H]\{V_z\} - [H_{yz}]\{V_y\} + [H_{zx}]\{V_x\} - [D_y]\{W_x\} + [D_x]\{W_y\} \end{Bmatrix} = 0, \tag{22}$$

where $[n_x]$, $[n_y]$ and $[n_z]$ are diagonal matrices of unit normal vector components $\vec{n} = \{n_x, n_y, n_z\}$ for each boundary source point.

Next, we decompose the vorticity vector into two parts. In vector $\{W_i\}_\Gamma$ only boundary vorticity values are non-zero and in vector $\{W_i\}_{\Omega'}$ only domain vorticity values are non-zero

$$\{W_i\} = \{W_i\}_\Gamma + \{W_i\}_{\Omega'}. \tag{23}$$

We include Eqs. (23) into (22) and reorder the result in such manner, that only boundary vorticity values are unknown on the left-hand side of the equation

$$\begin{aligned}
&([n_x][D_x] + [n_y][D_y] + [n_z][D_z])\{W_x\}_\Gamma \\
&\quad = ([n_y][H_{zx}] + [n_z][H_{xy}])\{V_x\} - ([n_z][H] + [n_y][H_{yz}])\{V_y\} \\
&\qquad + ([n_y][H] - [n_z][H_{yz}])\{V_z\}) + [n_x][D_x]\{W_x\}_\Gamma \\
&\qquad + [n_y][D_x]\{W_y\}_\Gamma + [n_z][D_x]\{W_z\}_\Gamma \\
&\qquad - ([n_y][D_y] + [n_z][D_z])\{W_x\}_{\Omega'} \\
&\qquad + [n_y][D_x]\{W_y\}_{\Omega'} + [n_z][D_x]\{W_z\}_{\Omega'}, \\
&([n_x][D_x] + [n_y][D_y] + [n_z][D_z])\{W_y\}_\Gamma \\
&\quad = ([n_z][H_{xy}] + [n_x][H_{yz}])\{V_y\} - ([n_x][H] + [n_z][H_{zx}])\{V_z\} \\
&\qquad + ([n_z][H] - [n_x][H_{zx}])\{V_x\}) \\
&\qquad + [n_x][D_y]\{W_x\}_\Gamma + [n_y][D_y]\{W_y\}_\Gamma \\
&\qquad + [n_z][D_y]\{W_z\}_\Gamma - ([n_z][D_z] + [n_x][D_x])\{W_y\}_{\Omega'} \\
&\qquad + [n_z][D_y]\{W_z\}_{\Omega'} + [n_x][D_y]\{W_x\}_{\Omega'}, \\
&([n_x][D_x] + [n_y][D_y] + [n_z][D_z])\{W_z\}_\Gamma \\
&\quad = ([n_x][H_{yz}] + [n_y][H_{zx}])\{V_z\} \\
&\qquad - ([n_y][H] + [n_x][H_{xy}])\{V_x\} + ([n_x][H] - [n_y][H_{xy}])\{V_y\}) \\
&\qquad + [n_x][D_z]\{W_x\}_\Gamma + [n_y][D_z]\{W_y\}_\Gamma \\
&\qquad + [n_z][D_z]\{W_z\}_\Gamma - ([n_x][D_x] + [n_y][D_y])\{W_z\}_{\Omega'} \\
&\qquad + [n_x][D_z]\{W_x\}_{\Omega'} + [n_y][D_z]\{W_y\}_{\Omega'},
\end{aligned} \tag{24}$$

where subscript Γ stands for boundary nodes only and Ω' stands for interior nodes only (without boundary nodes). Eq. (24) gives three systems of linear equations, each of size $N_\Gamma \times N_\Gamma$.

4.2. Discrete form of FEM kinematics

We use Eq. (24) only for computation of boundary vorticities. To obtain internal velocities we use the same kinematic Eq. (4) but this time we use finite element method to discretise it, using $\vec{\omega}$ obtained by BEM as boundary condition.

The use of interpolation functions N as weighting functions and replacement of continuous functions with discrete ones (17) in Eq. (12), leads us to

$$\begin{aligned}
([D] - [B])\{V_x\} &= [G_y]\{W_z\} - [G_z]\{W_y\}, \\
([D] - [B])\{V_y\} &= [G_z]\{W_x\} - [G_x]\{W_z\}, \\
([D] - [B])\{V_z\} &= [G_x]\{W_y\} - [G_y]\{W_x\},
\end{aligned} \tag{25}$$

with

$$D^{in,jn} = \sum_{e=1}^{ne} \int_{\Omega_e} \frac{\partial N_{in}}{\partial x_i} \frac{\partial N_{jn}}{\partial x_i} \, d\Omega, \tag{26}$$

$$B^{in,jn} = \sum_{e=1}^{ne} \int_{\Gamma_e} N_{in} \left(\frac{\partial N_{jn}}{\partial x_i} n_i \right) d\Gamma, \tag{27}$$

$$G_i^{in,jn} = \sum_{e=1}^{ne} \int_{\Omega_e} N_{in} \frac{\partial N_{jn}}{\partial x_i} \, d\Omega, \tag{28}$$

where i is coordinate axis index, $\{V_i\}$ and $\{W_i\}$ are nodal velocity and vorticity vector in domain Ω, $[D]$ is diffusion matrix, $[B]$ is boundary flux matrix and $[G_i]$ is gradient matrix. Indices in and jn are the row and column position of integral in matrix (node numbers of the source and destination node in discretised domain) and n_i is outward pointing unit normal vector.

4.3. Discrete form of FEM vorticity transport equation

Similarly, the discrete form of kinetic vorticity transport equation is obtained by using Eq. (17) in Eq. (15) leading to the next vector equation

$$\begin{aligned}
&\left(\frac{1}{\Delta t}[M] + [C] + \nu[D] - \nu[B] \right)\{W_i\} \\
&\quad = [V_{i,j}]\{W_j\} + \frac{1}{\Delta t}[M]\{W_i\}_{\tau-1},
\end{aligned} \tag{29}$$

with

$$M^{in,jn} = \sum_{e=1}^{ne} \int_{\Omega_e} N_{in} N_{jn} \, d\Omega, \tag{30}$$

$$C^{in,jn} = \sum_{e=1}^{ne} \int_{\Omega_e} N_{in}\left(v_i \frac{\partial N_{jn}}{\partial x_i}\right) \mathrm{d}\Omega, \tag{31}$$

$$V_{i,j}^{in,jn} = \sum_{e=1}^{ne} \int_{\Omega_e} N_{in}\left(\frac{\partial v_i}{\partial x_j} N_{jn}\right) \mathrm{d}\Omega, \tag{32}$$

where $\{W_i\}$ is nodal vorticities vector in domain Ω, $\{W_i\}_{\tau-1}$ are nodal values of vorticity in previous time step and $[M]$, $[C]$ and $[V_{i,j}]$ are mass, convection and vortex twisting and stretching matrix. $[D]$ and $[B]$ are diffusion and boundary flux matrices defined in previous section.

With application of boundary conditions in Eqs. (25) and (29) the final systems of linear equations can be obtained.

5. Computational algorithm

The solution algorithm can be described as follows:

(1) Choose initial velocity ($\vec{v}_0$) field, compute initial vorticity ($\vec{\omega}_0$) field using Eq. (3), set initial time level $\tau = 0$, set initial nonlinear iteration level $i = 0$.
(2) Time loop, $\tau \coloneqq \tau + 1$.
(3) Nonlinear iteration loop, $i \coloneqq i + 1$.
(4) Flow kinematics:
  (a) Solve Eqs. (24) by BEM for boundary vorticities, using internal vorticities from previous nonlinear iteration step.
  (b) Solve Eqs. (25) by FEM for domain velocities, using new boundary vorticities to form right-hand side vector. It is also possible to use explicit BEM calculation, however this requires calculation and storage of a large number of integrals. Due to limited computer memory, we used FEM instead.
(5) Flow kinetics, vorticity transport:
  (a) Solve Eqs. (29) by FEM for domain vorticities, using the new velocity field to obtain the convection matrix (31) and use boundary vorticities from kinematics as boundary conditions.
  (b) Use underrelaxation $0 < \phi \leqslant 1$ for computing new domain vorticity values $\vec{\omega}_{i+1} \coloneqq \phi\vec{\omega}_{i+1} + (1-\phi)\vec{\omega}_i$.
(6) Check convergence:
  (a) Compute $error = \|\vec{\omega}_{i+1} - \vec{\omega}_i\|_2 / \|\vec{\omega}_{i+1}\|_2$.
  (b) If *error* is greater then predefined ε go to step 3.
(7) Finish time loop:
  (a) Store time step values $\vec{\omega}_\tau = \vec{\omega}_{i+1}$, $\vec{v}_\tau = \vec{v}_{i+1}$.
  (b) If time step τ is less than maximum number of time steps NT go to step 2.
(8) End of computation.

Different types of system of linear equations (SLE) solvers were used in the computation, depending on the SLE structure (full or sparse). For the full systems, the direct solver with lower–upper (LU) decomposition or the iterative solver with diagonal preconditioning were used, depending on whether the computation was performed in serial or parallel. Sparse systems were solved using iterative solver with incomplete LU decomposition. Iterative solver used was BiCGSTAB(L), see Sleijpen and Fokkema [20], with prescribed tolerance $slv_{eps} = 10^{-6}$.

Computer code was compiled using Intel fortran 90 compiler 8.1 with −O3 optimisation. Computation was done on IBM Linux Cluster 1350 with 512 dual Xeon 3.0 GHz processors with 2 GB of memory per node and SuSE SLES 8 Linux operating system with smp kernel 2.4.21.

6. Lid driven cavity

Lid driven cavity flow is one of the standard benchmark test cases for laminar viscous fluid flow. It possesses some very favorable properties, namely very unambiguous boundary conditions, unchanged flow domain when Reynolds number value is increased and last but not least it exhibits almost all phenomena that can possibly occur in incompressible flows: eddies, secondary flows, complex three-dimensional patterns, chaotic particle motions, instabilities, transition and turbulence [21].

Hardly any work existed on the topic until the pioneering experimental work of Koseff and Street

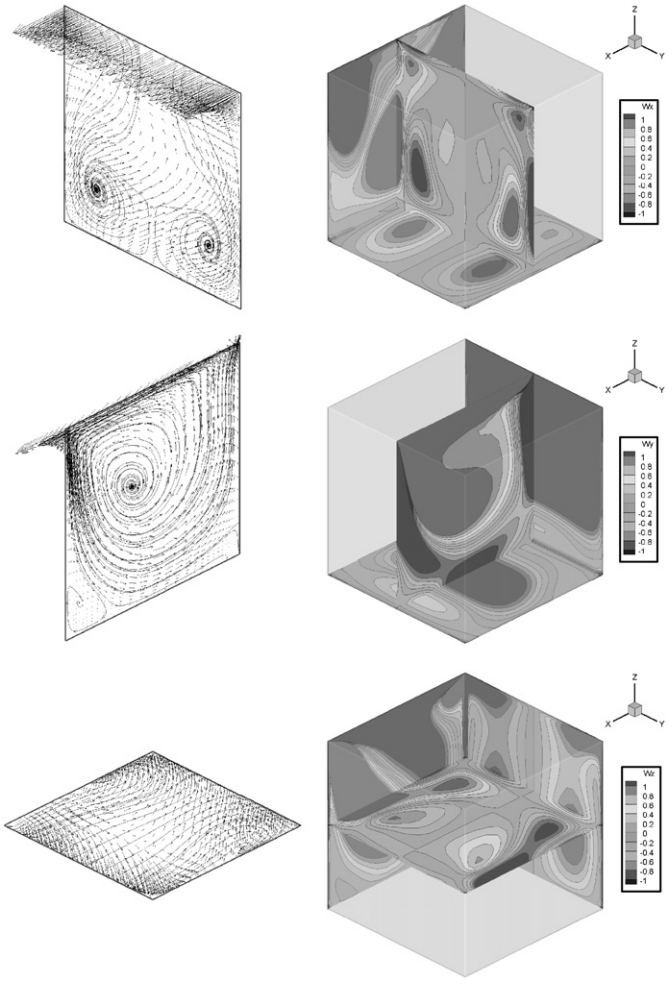

Fig. 1. Velocity vectors, stream traces and vorticity contours in different planes of the cavity, $Re = 400$.

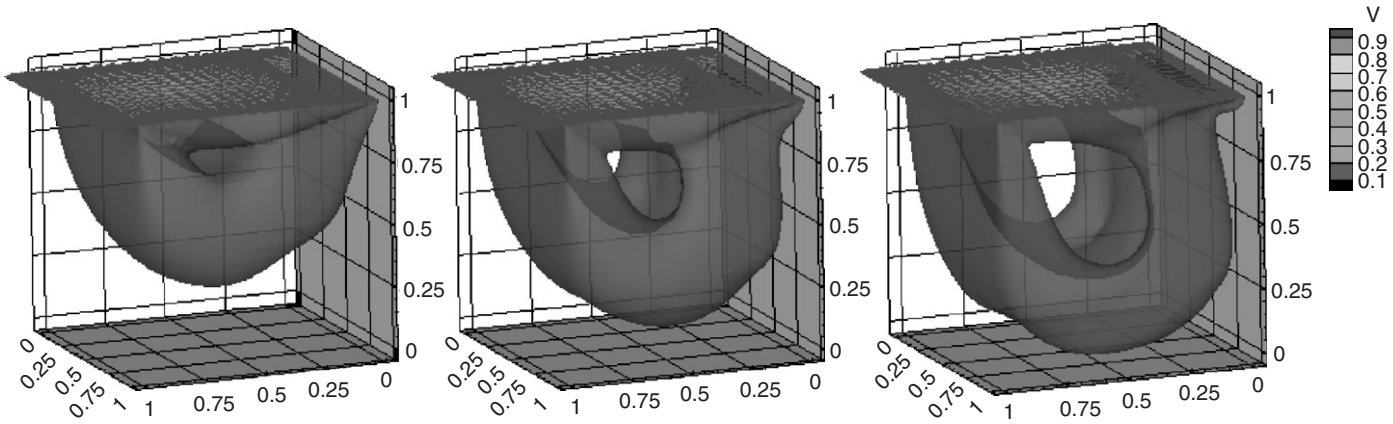

Fig. 2. Isosurface of magnitude of velocity $|\vec{v}| = 0.13$ for different Reynolds number values, $Re = 100$ left, $Re = 400$ middle and $Re = 1000$ right.

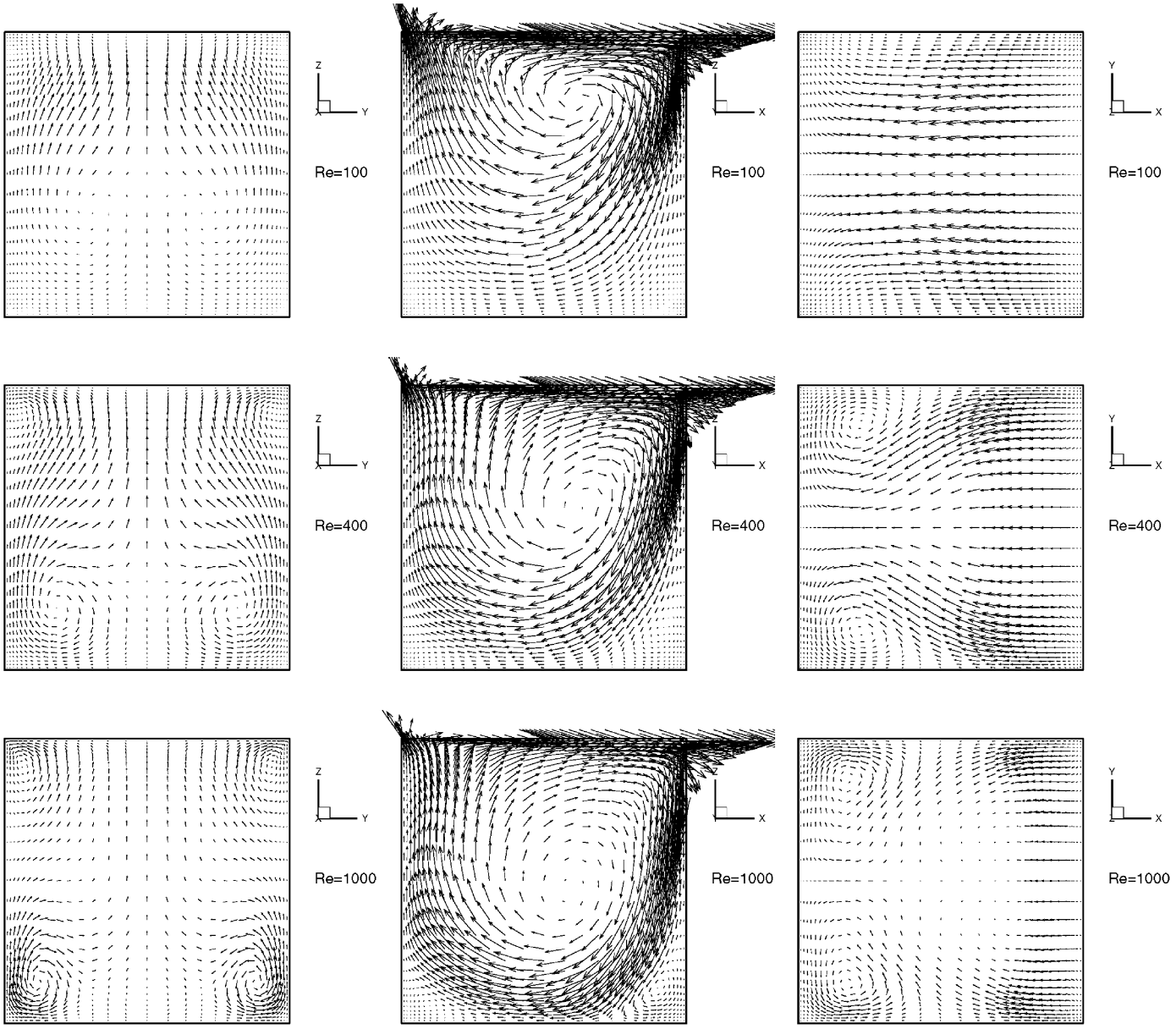

Fig. 3. Velocity vectors on center-planes for different Reynolds number values.

[22–24]. Their studies, however, changed the whole picture because they clearly showed that cavity flows were inherently 3-D in nature. Not only are 2-D models inadequate, they can be seriously misleading as stressed out by Shankar and Deshpande [21].

In our computation we used a cubic cavity with the edge size $L = 1$. The Reynolds number, the only dimensionless number in this case, is based on the cavity's edge size and the top lid velocity, $Re = v_x L/\nu$, and was selected to be $Re = 100$, 400 and 1000.

The mesh size used were $8 \times 8 \times 8$, $16 \times 16 \times 16$ and $32 \times 32 \times 32$ elements ($9 \times 9 \times 9$, $17 \times 17 \times 17$ and $33 \times 33 \times 33$ expressed with nodes), all with maximum to minimum element length ratio of 8, with elements clustered near the walls.

Velocity boundary conditions were:

- $z = 1$: moving wall ($v_x = 1$, $v_y = v_z = 0$),
- $x = 0$, $x = 1$, $y = 0$, $y = 1$, $z = 0$: no slip ($v_x = v_y = v_z = 0$).

Prescribed convergence criterium for nonlinear iterations was $\varepsilon = 1 \times 10^{-6}$. Test cases with $Re = 100$ and 400 were computed with time step $\Delta t = 2\,\mathrm{s}$ and underrelaxation factor $\phi = 0.2$, test case with $Re = 1000$ was computed with time step $\Delta t = 0.2\,\mathrm{s}$ and underrelaxation factor $\phi = 0.2$.

All test cases were computed with initial conditions of $v_x = v_y = v_z = 0$. Prescribed tolerance for iterative solver was $\varepsilon_{slv} = 10^{-6}$. Results were compared to the results of Yang et al. [25].

For the prescribed time step size the test case on the finest mesh for $Re = 100$ needed 15 time steps to reach steady state, for $Re = 400$, 28 time steps and $Re = 1000$, 375 time steps.

Fig. 1 shows 3-D sectional perspective views for the computed velocity vector and vorticity fields for $Re = 400$. The vorticity plots at x-mid-plane for ω_x, y-mid-plane for ω_y and z-mid-plane for ω_z fully illustrate the developed vorticity field.

Fig. 2 shows isosurfaces of absolute velocity $|\vec{v}| = \sqrt{v_x^2 + v_y^2 + v_z^2} = 0.13$ for different Reynolds number values. It can be seen, that the high speed core of the fluid becomes narrower with the increasing of the Reynolds number value.

Fig. 3 shows comparison of velocity vectors on center-planes for different Reynolds number values.

It can be seen that in the z–y planes a pair of vortices appear near the centerline of the cavity and move out towards the lower corners as the Reynolds number increases. Additional two vortices appear in the top corners at $Re = 1000$. In the x–y plane, fluid at first flows uniformly backwards and with the increasing of the Reynolds number value two vertical vortices appear.

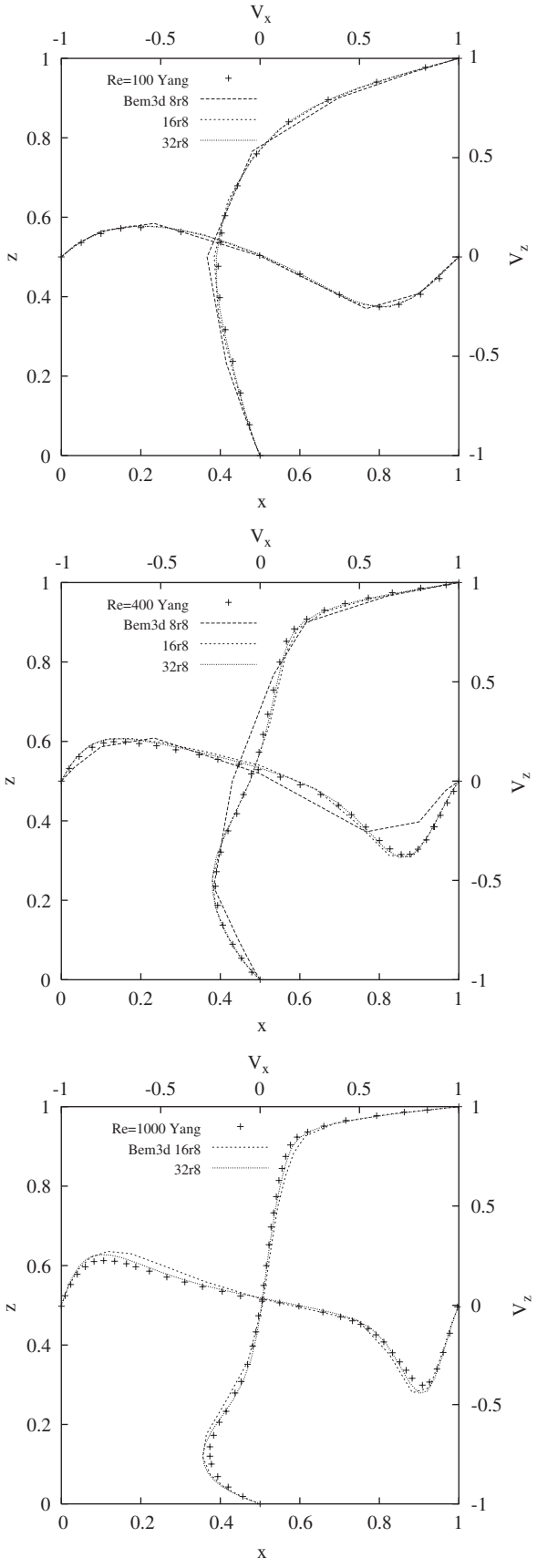

Fig. 4. Velocity profiles along centerlines for different mesh sizes, $Re = 100$ top left, $Re = 400$ top right and $Re = 1000$ bottom.

Similar behavior of the velocity field was reported also by Wong and Baker [4].

The quantitative evaluation of the results is shown in Fig. 4, where we compare the v_x velocity along $x = y = 0.5$ centerline and v_z velocity along $y = z = 0.5$ centerline for different mesh sizes and different Reynolds number values. The mesh refinement shows that the coarsest mesh is too coarse, although it gives qualitatively reasonable results. The finest two meshes are in close agreement with the benchmark solution of Yang et al. [25].

7. Conclusions

A new approach to the numerical solution of Navier–Stokes equations in velocity–vorticity formulation was presented. It consists of implicit calculation of boundary vorticities by means of boundary element method and calculation of vorticity transport by means of finite element method. For the computation of internal velocities the approach of solving the implicit system of equations, resulting from the finite element method discretisation of elliptic Poisson velocity equation was used. Well known lid driven cubic cavity test case was used to test the accuracy of the proposed method. Numerical testings showed, that the proposed combination of BEM and FEM is a promising computational tool for the numerical solution of 3-D incompressible Navier–Stokes equations.

Acknowledgments

The work has been partially performed under the Project HPC-EUROPA (RII3-CT-2003-506079), with the support of the European Community—Research Infrastructure Action under the FP6 "Structuring the European Research Area" Programme.

References

[1] Liu CH. Numerical solution of three-dimensional Navier–Stokes equations by a velocity–vorticity method. Int J Numer Meth Fluids 2001;35:533–57.
[2] Guevremont G, Habashi WG. Finite element solution of the Navier–Stokes equations by a velocity–vorticity method. Int J Numer Meth Fluids 1990;10:461–75.
[3] Guevremont G, Habashi WG, Kotiuga PL, Hafez MM. Finite element solution of the 3D compressible Navier–Stokes equations by a velocity–vorticity method. J Comput Phys 1993;107(1):176–87.
[4] Wong KL, Baker AJ. A 3D incompressible Navier–Stokes velocity–vorticity weak form finite element algorithm. Int J Numer Meth Fluids 2002;38:99–123.
[5] Žagar I, Škerget L. Boundary elements for time dependent 3-D laminar viscous fluid flow. J Mech Eng 1989;35(10/12):160–3.
[6] Hriberšek M, Škerget L. Iterative methods in solving Navier–Stokes equations by the boundary element method. Int J Numer Meth Eng 1996;39:115–39.
[7] Škerget L, Hriberšek M, Žunič Z. Natural convection flows in complex cavities by BEM. Int J Numer Meth Heat Fluid Flow 2003;13(6):720–35.
[8] Young DL, Huang JL, Eldho TI. Simulation of laminar vortex shedding flow past cylinders using a coupled BEM and FEM model. Comput Meth Appl Mech Eng 2001;190:5975–98.
[9] Young DL, Liu YH, Eldho TI. A combined BEM–FEM model for the velocity–vorticity formulation of the Navier–Stokes equations in three dimensions. Eng Anal Bound Elem 2000;24:307–16.
[10] Brown MJ, Ingber MS. Parallelization of a vorticity formulation for the analysis of incompressible viscous fluid flows. Int J Numer Meth Fluids 2002;39:979–99.
[11] Brown MJ, Mammoli AA, Ingber MS. Parallel multipole implementation of the generalized Helmholtz decomposition for solving viscous flow problems. Int J Numer Meth Eng 2003;58:1617–35.
[12] Žunič Z, Škerget L, Hriberšek M, Ravnik J. Boundary element–finite element method for velocity–vorticity formulation of Navier–Stokes equations. In: Brebbia CA, Carlomagno GM, editors. Computational methods and experimental measurements XII, vol. 41. Southampton, Boston: WIT Press; 2005. p. 793–802.
[13] Škerget L, Hriberšek M, Kuhn G. Computational fluid dynamics by boundary domain integral method. Int J Numer Meth Eng 1999;46:1291–311.
[14] Ramšak M, Škerget L, Hriberšek M, Žunič Z. A multidomain boundary element method for unsteady laminar flow using stream function–vorticity equations. Eng Anal Bound Elem 2005;29:1–14.
[15] Ravnik J, Škerget L, Hriberšek M. Two-dimensional velocity–vorticity based LES for the solution of natural convection in a differentially heated enclosure by wavelet transform based BEM and FEM. Eng Anal Bound Elem 2006;30:671–86.
[16] Wu JC, Thompson JF. Numerical solutions of time-dependent incompressible Navier–Stokes equations using an integro-differential formulation. Comput Fluids 1973;1:197–215.
[17] Wrobel LC. The boundary element method. New York: Wiley; 2002.
[18] Taylor C, Hughes TG. Finite element programming of the Navier–Stokes equations. Swansea, U.K.: Pineridge Press Ltd.; 1981.
[19] Gresho PM, Sani RL. Incompressible flow and the finite element method, vol. 1: advection–diffusion. New York: Wiley; 2000.
[20] Sleijpen GLG, Fokkema DR. BiCGSTAB(L) for linear equations involving unsymmetric matrices with complex spectrum. Electron Trans Numer Anal 1993;11:11–32.
[21] Shankar PN, Deshpande MD. Fluid mechanics in the driven cavity. Annu Rev Fluid Mech 2000;32:93–136.
[22] Koseff JR, Street RL. Visualization of a shear driven three-dimensional recirculating flow. J Fluids Eng 1984;106:21–9.
[23] Koseff JR, Street RL. On the endwall effects in a lid-driven cavity flow. J Fluids Eng 1984;106:385–9.
[24] Koseff JR, Street RL. The lid-driven cavity flow: a synthesis of qualitative and quantitative observations. J Fluids Eng 1984; 106:390–8.
[25] Yang JY, Yang SC, Chen YN, Hsu CA. Implicit weighted ENO schemes for the three-dimensional incompressible Navier–Stokes equations. J Comput Phys 1998;146:464–87.